Development 119, 909-919 (1993)
Printed in Great Britain © The Company of Biologists Limited 1993

Ultraviolet irradiation impairs epiboly in zebrafish embryos: evidence for a microtubule-dependent mechanism of epiboly

Uwe Strähle and Suresh Jesuthasan

Molecular Embryology Laboratory, Imperial Cancer Research Fund, Developmental Biology Unit, Department of Zoology, South Parks Road, Oxford OX1 3PS, UK

SUMMARY

Early morphogenesis of the teleost embryo is characterized by three orchestrated cell movements. Epiboly leads to spreading of the blastoderm over an uncleaved yolk cell while involution around the blastoderm margin and convergence movements towards the dorsal side generate the mes-endodermal inner cell sheet and the axis rudiment, respectively. Irradiation of zebrafish zygotes with ultraviolet light selectively impairs epiboly resulting in embryos with open blastopores but well-formed anterior axes. Gastrulation movements are only marginally affected by ultraviolet irradiation. Involution of marginal cells in epiboly-retarded embryos takes place prior to 50% epiboly and thus appears independent of epiboly. Expression of dorsal and anterior marker genes is unaffected by ultraviolet irradiation.

The ultraviolet light effect is not restricted to the zygote stage as irradiation of later embryonic stages also impairs epiboly. The ultraviolet-sensitive targets may thus be maternally encoded components of the machinery driving epiboly. These targets appear to be microtubules: firstly, irradiated embryos show disorganized and less microtubules in the cytoplasmic layer of the yolk sphere; secondly, the ultraviolet light effect can be mimicked by the microtubule-depolymerising agent nocodazole. We suggest that epiboly is driven, at least partially, by motors that use microtubules radiating from the yolk syncytial layer into the yolk cytoplasmic layer. Together with an observed constrictive behaviour of the blastoderm margin, we propose a two-force model of epiboly: epiboly is initiated and driven by a pulling force dependent on microtubules in the yolk cytoplasmic layer; contraction at the margin operates in addition to aid closure of the blastopore.

Key words: ultraviolet light, gastrulation, epiboly, microtubules, zebrafish

INTRODUCTION

The early teleost embryo is formed by three harmonized cell movements: epiboly, involution and convergence (Devillers, 1961; Ballard, 1973a; Trinkaus, 1984a,b; Wood and Timmermans, 1988; Warga and Kimmel, 1990). Meroblastic cleavage of the zygote results in a densely packed cap of cells sitting at the animal pole of an uncleaved sphere of yolk. This cap, the blastoderm, subsequently spreads evenly over the yolk mass in the process of epiboly (Trinkaus, 1984a,b). In the zebrafish, involution commences when the spreading blastoderm has reached the equator of the yolk sphere (Warga and Kimmel, 1990). Deep cells around the margin of the blastoderm involute and migrate up towards the animal pole giving rise to the hypoblast from which mesodermal and endodermal organs derive (Kimmel et al., 1990; Warga and Kimmel, 1990). At the same time, both involuted and non-involuted deep cells converge to the dorsal side of the embryo to form the embryonic shield, which is the primordium of the body axis (Warga and Kimmel, 1990). Epiboly continues as deep cells involute and converge. Ultimately, these movements result in a yolk sphere completely covered by the blastoderm with the future body axis visible as a distinct thickening on the dorsal side of the embryo.

Convergence and involution are the result of active migration of individual deep cells that move between the outer enveloping layer of cells and the inner yolk syncytial layer (Fig. 1) (Warga and Kimmel, 1990; Trinkaus, 1992). Deep cells move presumably utilizing mechanisms employed by other locomoting cells such as fibroblasts: when observed in living *Fundulus* embryos, moving deep cells extend filopodia and lamellipodia (Trinkaus and Erickson, 1983). Epiboly, on the other hand, appears to be based on a completely different mechanism. Cells at the advancing edge do not extend protrusions, suggesting that the blastoderm does not actively crawl over the surface of the yolk (Betchaku and Trinkaus, 1978). Instead, it appears to be carried over the yolk by the yolk syncytial layer (Trinkaus, 1984a, 1992). This multi-nuclear cytoplasmic layer, which arises by the collapse of marginal blastomeres into the yolk cell (Kimmel and Law, 1985), epibolizes ahead of the blastoderm; it is even able to complete epiboly when the blastoderm is removed (Trinkaus, 1951). The enveloping layer is firmly attached by tight and close junctions to the yolk syncytial layer (Betchaku and Trinkaus, 1978) and

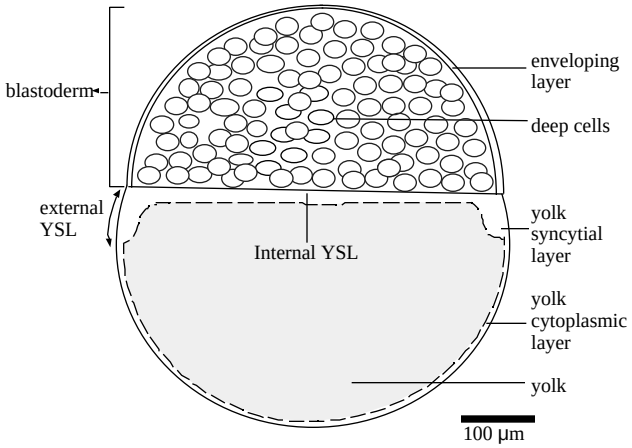

Fig. 1. Schematic cross section through an early zebrafish embryo, showing the various cell types present during early epiboly and gastrulation. YSL, yolk syncytial layer.

thereby encloses the deep cells. If its attachments to the yolk syncytial layer are broken, the blastoderm springs back while the yolk syncytial layer spreads over the yolk at an increased rate, implying that the yolk syncytial layer pulls the blastoderm during epiboly (Trinkaus, 1951; Betchaku and Trinkaus, 1978). The molecular nature of the mechanism driving advance of the yolk syncytial layer, and therefore epiboly, remains a mystery.

Here, we show that epiboly in zebrafish embryos is selectively impaired by irradiating zygotes with ultraviolet light (UV). Gastrulation movements by the deep cells are only marginally affected by the UV treatment and embryos with a well-formed anterior axis are obtained regularly. Gastrulation commences at the same time in treated and untreated siblings, indicating that the timing of gastrulation movements is independent of the degree of epiboly. Two lines of evidence suggest that UV irradiation impairs epiboly by disrupting microtubules: firstly, prominent arrays of microtubules are present in the yolk cytoplasm during normal development and these are disorganized in irradiated embryos. Secondly the microtubule-depolymerizing drug nocodazole mimics the effect of UV irradiation. We thus propose that epiboly is driven by a mechanism dependent on microtubules in the yolk cytoplasm.

MATERIALS AND METHODS

Fish rearing and embryo culture

Zebrafish were obtained from a pet shop. Fish and embryos were maintained as described (Westerfield, 1993).

UV irradiation and nocodazole treatment

Embryos from natural spawings were exposed randomly oriented in their chorion to UV light in a home-made cuvette. The cuvette was constructed from a cut-off scintillation vial to which a UV-transparent quartz disc (Jenson) was glued. The cuvette was placed on a 254 nm UVP 54 mineral light (UVP, Cambridge). UV doses were varied by changing exposure times. After irradiation, embryos were transfered into embryo medium (Westerfield, 1993) and kept at 28.5°C. UV doses were measured with a UV meter (UVP, Cambridge) by placing the sensor directly onto the UV source.

Embryos at cleavage stages, between the 16- and 128-cell stage, were dechorionated with watchmakers forceps and exposed to nocodazole (Aldrich). A stock solution of 2 mg/ml nocodazole in DMSO (BDH Chemicals) was diluted in 10% Hank's saline to give working concentrations between 0.6 µg/ml and 2.0 µg/ml. The drug was washed out after 10 minutes by rinsing the embryos several times in fresh 10% Hank's.

Tracking of cells and microscopy of living embryos

One blastomere of 32-cell-stage embryos was injected with TRITC-dextran (Molecular Probes, Oregon) using a gas-pressure injector. Embryos were kept at 28.5°C to develop until control embryos were near 50% epiboly. Embryos were mounted in an observation chamber in which the coverslip was supported by 5 layers of electrical tape giving a thickness of 0.65 mm, then examined every 10 minutes with a confocal microscope (MRC600, Biorad).

A Leitz Diaplan with differential interference contrast optics or a Zeiss stereo microscope was employed for documentation of embryos.

In situ hybridisation and immunochemistry

Fixation of embryos and in situ hybridisation with digoxigenin-labelled antisense RNA probes were carried out as described (Strähle et al., 1993). Immuno-staining with the zebrafish anti-notail (Brachyury, ZF-T) antibody was reported recently (Schulte-Merker et al., 1992).

For staining with the anti-β-tubulin antibody, embryos were fixed in microtubule-stabilizing buffer (Schroeder and Gard, 1992) for 5 hours at room temperature. They were then transferred to 100% methanol and kept at 4°C overnight. Embryos were rehydrated to phosphate-buffered saline (PBS) and incubated overnight in a 1/500 dilution of anti-β-tubulin antibody (Amersham). After several washes in PBS, bound anti-β-tubulin antibody was reacted overnight with a FITC-conjugated secondary antibody in PBS containing 1% bovine serum albumin. After multiple washes in PBS, embryos were examined with a confocal microscope.

RESULTS

Effects of UV irradiation of zebrafish zygotes

Zygotes with well-formed blastodiscs, approximately 10 minutes before the first cleavage, were irradiated with short-wave UV (254 nm, 1.8 mJ/cm^2). Embryos were scored for defects at 12 hours of development. The results are summarized in Fig. 2 and Table 1. The UV-treated embryos could be grouped into three classes (Table 1). The majority, which we call type-A, showed impaired epiboly;

Table 1. Effects of UV irradiation on zebrafish zygotes

	UV	Normal	Type-A	Type-B	Type-C	Viability
Exp I	−	33	0	0	0	97%
	+	3	73	4	0	92%
Exp II	−	74	0	0	0	63%
	+	10	128	12	15	61%

Zebrafish zygotes were irradiated with UV light (Exp I, 1.8 mJ/cm^2; ExpII, 3.6 mJ/cm^2) and embryos scored for defects 12 hours after fertilisation. Zygotes were obtained from natural spawnings. Irradition was approximately 30 +/- 10 minutes after fertilisation. The viability count includes also unfertilized eggs.

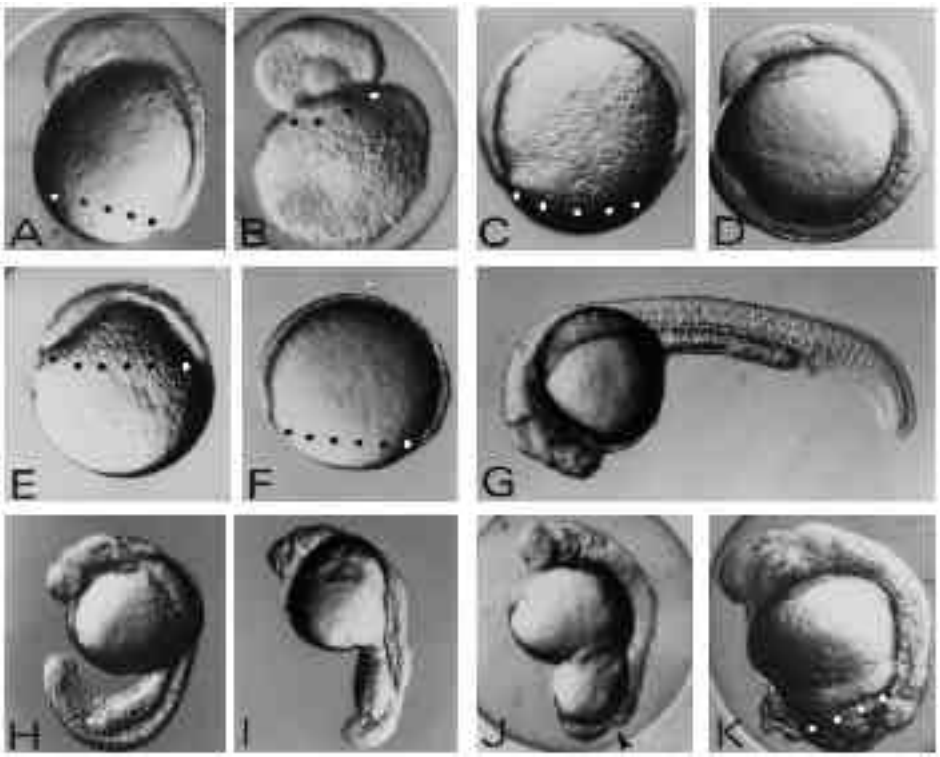

Fig. 2. Effects of UV exposure on zebrafish embryos. (A-D) The three classes of embryos generated by UV exposure of zygotes (A-C) and an untreated control embryo (D) at 12 hours of development. In the type-A embryo (A) the blastoderm has covered the yolk cell up to 80% and shows a well-formed anterior axis rudiment on the dorsal side. In type-B embryos (B) the blastoderm rounded up forming a vesicle on top of the yolk mass. Type-C embryos (C) show retardation of epiboly but do not form an axis rudiment. (E,F) UV-treated (E) and control embryo (F) at 8 hours of development. UV treatment results in strong retardation of epiboly. Control embryos (F) are at the 80% epiboly stage, whereas UV-exposed embryos (E) have just covered the yolk sphere by 40% at 8 hours after fertilisation. (G-K) UV-irradiated embryos (H-K) and a control embryo (G) at 24 hours of development. UV-treated embryos at this stage show various degrees of posterior defects ranging from subtle tail defects (H,I) to complete failure to finish epiboly (J,K) leaving the yolk cell uncovered by the blastoderm at the vegetal pole. The arrowhead in J indicates the open blastopore. Embryos were exposed to 1.8 mJ/cm^2 at the late zygote stage. Blastoderm margins are indicated by black or white dots. Embryos are oriented anterior up and dorsal to the right with the exception of panel G where anterior is to the left and dorsal up.

the yolk cell was covered on average only up to 80% by the blastoderm, leaving the yolk mass exposed at the vegetal pole (Fig. 2A). Untreated control embryos (Fig. 2D) have long finished epiboly by this time. The rapid succession of cleavages characteristic of early development of the zebrafish is not affected by UV treatment. The first effects of UV treatment become apparent with the onset of epiboly: treated embryos initiate and progress through epiboly slower than untreated controls (compare Fig. 2E and F). This suggests that UV-sensitive components of the machinery driving epiboly are present in the late zygote. As zygotic transcription is believed to begin only after the midblastula transition at 3 hours of development (Kane et al., 1992), the targets inactivated by UV are likely of maternal origin. Anterior axis formation does not seem to be affected in UV-treated embryos. Morphogenesis of brain, eyes, notochord and somites in type-A embryos appears to occur on schedule in comparison to controls of the same age. As a result, UV embryos form well-structured axes on incompletely covered yolk cells (compare Fig. 2A,D and F).

When observed at 12 hours of development, two other types of embryos were obtained irregularly, with much lower frequency than type-A embryos (Table 1). Type-B embryos (Fig. 2B) are characterised by a blastoderm that has pinched off the yolk cell, forming a vesicle resting on the disintegrating yolk mass. Type-C embryos (Fig. 2C) show retardation of epiboly but do not form a well-developed axis. Early irradiation of embryos, between 10 and 25 minutes after fertilization, caused an increase in the frequency of type-C embryos.

Most of the type-A embryos eventually close the blastopore showing that epiboly is only impaired and not completely blocked by a UV dose of 1.8 mJ/cm^2. Fig. 2G-K summarize the results at 24 hours of development. UV embryos of this age show impaired tail development to various degrees (Fig. 2H-K in comparison to control Fig. 2G). It seems that tail development requires closure of the blastopore as only embryos that succeeded in closing the blastopore show a tail rudiment (Fig. 2H,I). A smaller percentage of UV embryos failed to close the blastopore entirely (Fig. 2J,K). These embryos show varying additional defects ranging from yolks distorted into a peanut shape (Fig. 2J) to strongly undulating axes (see Fig. 6G), or even axes that are split at the posterior end.

UV treatment results in a dose-dependent retardation of epiboly

UV-treated embryos progress through epiboly slower than untreated siblings. To quantitate the effect of UV exposure on epiboly, we determined the velocity of epiboly in UV-treated (3.6 mJ/cm^2) and untreated embryos. The results are shown in Fig. 3A. Each point in the graph represents the average percentage epiboly determined from a randomly selected set of embryos at the times indicated. We measured the percentage of the yolk cell covered by the blastoderm (using a linear scale from 0% to 100% epiboly) rather than the actual distance travelled by the blastoderm margin over

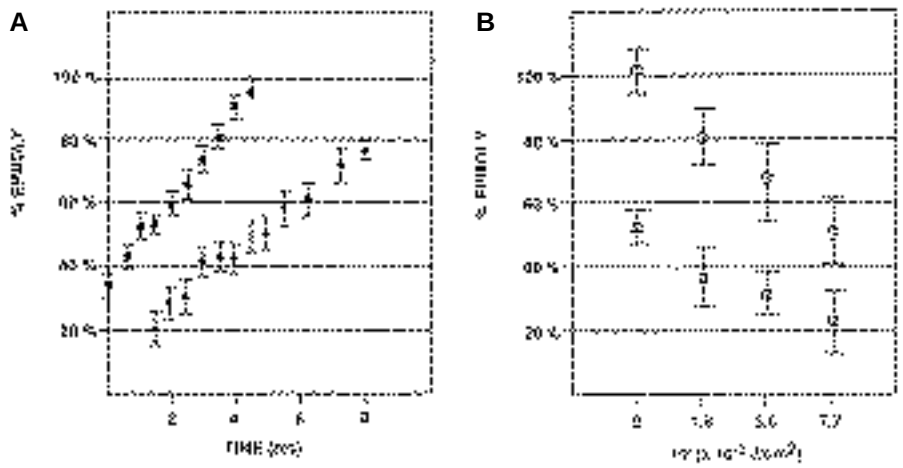

Fig. 3. Epiboly retardation and UV dose dependence. (A) Embryos were UV irradiated (3.6 mJ/cm^2) at the 1-cell stage and the degree of epiboly was monitored at various times after onset of epiboly in UV-treated (●) and control embryos (■). Each time point represents the average of multiple measurements (n=20-30). Standard deviations are indicated by bars. (B) Embryos at the 1-cell stage were exposed to UV light for varying times and the degree of epiboly was determined at the times when controls had reached either 50% epiboly (□) or 100% epiboly (○). Each point is the average of several measurements (n=20-30) and standard deviations are indicated by bars.

the yolk sphere. Epiboly starts later in UV-treated embryos and is slightly less synchronized than in control embryos. The speed of epiboly is reduced by UV irradiation. The blastoderm margin spreads with a speed of 15.2±0.6% epiboly/hour (mean ± s.d.) over the yolk in controls, whereas the speed of epiboly is reduced to 7.5±0.4% epiboly/hr (mean ± s.d.) in UV-irradiated embryos.

We next wished to determine whether retardation of epiboly is dependent on the UV dose applied. Embryos at the late 1-cell stage were exposed to various doses of UV and the degree of epiboly was measured in randomly selected sets of embryos from each of the differently exposed batches, at times when control embryos had reached approximately 50% and 100% epiboly. The results are shown in Fig. 3B. Increasing doses of UV led to a linear increase in retardation of epiboly. Higher doses did not result in a significant increase of lethality, at least up to the times when the degree of epiboly was scored. The frequency of type-B embryos, however, increased with increasing doses.

Retardation of epiboly by UV irradiation of late zygote stages suggests that components of the machinery driving epiboly are already present in the zygote. If this is true, exposure of older embryos to UV light should also result in impaired epiboly. Cleavage- (16-cell-stage) and mid-epiboly-stage embryos were treated with UV light and examined for the degree of yolk cell coverage at the time when untreated control embryos had reached the 4-somite stage. The results are summarized in Table 2 and representative embryos are shown in Fig. 4. UV irradiation (3.6 mJ/cm^2) of 16-cell-stage embryos had the same effect on epiboly as exposure of zygotes (Fig. 4A) showing that the UV effect on epiboly is not confined to the zygote stage. Irradiation of 50% epiboly stage embryos also led to retardation of epiboly. Due to relatively late application of UV, the retardation is not quite as pronounced as in embryos irradiated at the 16-cell stage (Fig. 4B, blastopore about to be closed). This stage independence of the UV effect on epiboly supports the notion that UV disrupts a component of the motor driving epiboly.

Table 2. UV irradiation of embryos at the 16-cell and 50% epiboly stage

Stage	UV	Normal	Type-A	Type-B	Type-C	Viability
16 cell	−	59	0	0	0	98%
	+	2	40	1	0	98%
50% Epiboly	−	18	0	0	0	100%
	+	0	19	0	0	76%

Embryos at the 16-cell or the 50% epiboly stage were irradiated with UV light (1.8 mJ/cm^2) and scored for induction of type-A, type-B and type-C embryos.

Involution and convergence movements in UV embryos

In normal zebrafish development, gastrulation movements leading to the formation of the hypoblast and the embryonic shield invariably start when 50% of the yolk cell is covered by the spreading blastoderm. Embryos exposed to high

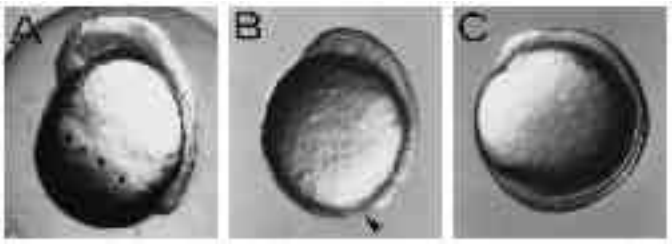

Fig. 4. Retardation of epiboly by UV exposure is stage-independent. Embryos at 16-cell (A) or 50% epiboly stage (B) were exposed to UV light (2.7 mJ/cm^2) and cultivated until untreated control embryos (C) had reached the 4-somite stage. Blastoderm margin is indicated by dots. The embryo in B has just closed the blastopore (pointed out by an arrowhead). Embryos are oriented anterior up and dorsal to the right.

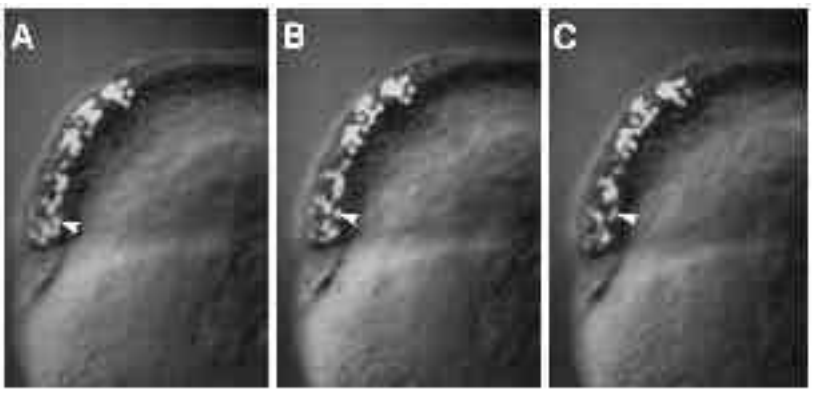

Fig. 5. Initiation of gastrulation is independent of the degree of epiboly. In this UV-treated embryo at the 30 % epiboly stage, a labeled involuted cell (arrowhead) is seen migrating upwards towards the animal pole. Untreated controls (not shown) were at the 50% epiboly at this time and had also begun involution. The frames shown were taken at 10 minute intervals. The embryos were irradiated at early cleavage stages and then labeled by injecting a single blastomere at the 32-cell stage with TRITC-dextran. Animal poles are up, the dorsal side could not be identified at these early involution stages.

doses of UV show prominent embryonic shields, even though the blastoderms in these embryos cover less than 50% of the yolk cell. This suggests that involution and convergence movements are initiated prior to the 50% epiboly stage. To observe cell movements directly, we injected TRITC-dextran into one blastomere of 32-cell UV-treated embryos and followed the migratory behaviour of the labeled cells during early epiboly stages. As shown in Fig. 5, cells involute and migrate upwards towards the animal pole in UV embryos that are only at 30% epiboly. Untreated siblings are at 50% epiboly at this time, suggesting that UV-treated embryos start involution at the same time as untreated embryos. Initiation of gastrulation therefore appears to be independent of the position of the blastoderm margin on the yolk cell; involution of marginal cells seems to be timed by an epiboly-independent clock.

To assess whether these early involuting cells also express genes characteristic for gastrulation stages, we carried out in situ hybridisation experiments on UV-treated and control embryos with axis-specific gene probes. The *Axial* gene is expressed in normal embryos in the fish organizer region at the dorsal blastoderm margin just before gastrulation starts (Strähle et al., 1993). During gastrulation, expression extends as a narrow stripe along the dorsal midline in mesendodermal cells. At the end of gastrulation (90% epiboly), expression is also turned on along the midline of the neural plate (Strähle et al., 1993). As shown in Fig. 6A, *Axial* is expressed in UV-treated embryos at the 30% epiboly stage. The expression pattern resembles that of an untreated sibling of the same age that has reached 50% epiboly (Fig. 6B). *Axial* expression in untreated embryos was never observed to occur before 40% epiboly (Strähle et al., 1993). In UV-treated embryos at the 50% epiboly stage, *Axial*-expressing cells have spread in the involuting hypoblast towards the

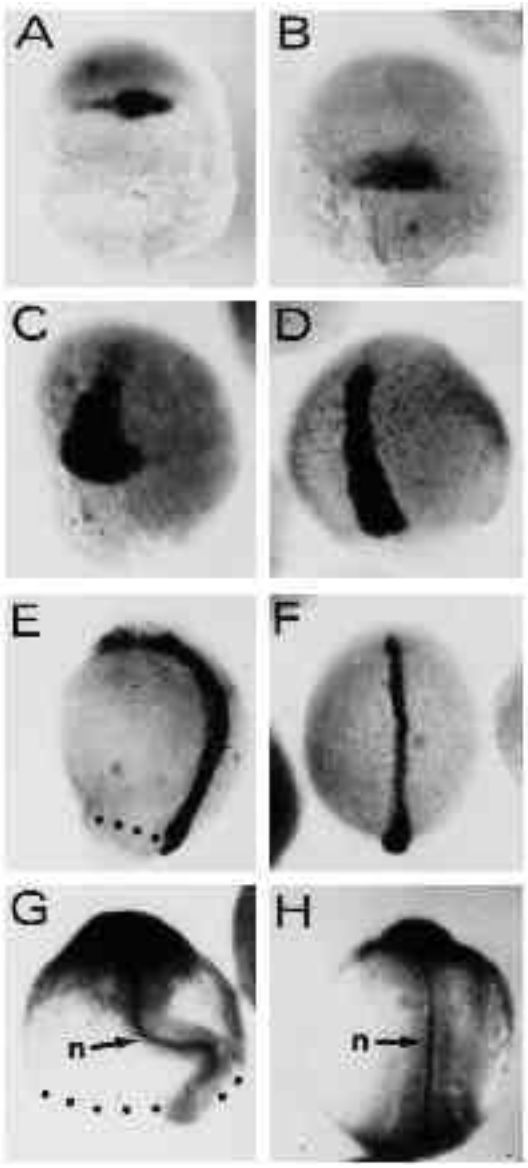

Fig. 6. Expression of dorsal gene markers is unaffected by UV treatment in type-A embryos. Embryos were hybridized with a digoxigenin-labeled antisense RNA probe complementary to the *Axial* gene RNA (A-F) or stained with the anti-ntl (zebrafish Brachyury, ZF-T) antibody (G,H). (A,B) UV-retarded embryo at 30% epiboly and control embryo at 50% epiboly stage, respectively. *Axial* expression marks the region of the fish organizer. (C,D) UV embryo at 50 % epiboly and untreated control at 80% epiboly, respectively. *Axial* -postive cells have involuted and spread towards the animal pole along the dorsal midline of the embryos. (E,F) UV-retarded and control embryo, respectively. Control embryo is at the 4-somite stage. (G,H) 14-hour embryos stained with the anti-ntl antibody. Embryo in G was UV treated. (H) An untreated control embryo. The notochord is indicated by n. Embryos were UV treated at early cleavage stages (3.6 mJ/cm^2). Blastoderm margins are indicated by dots. Orientation of embryos is anterior up.

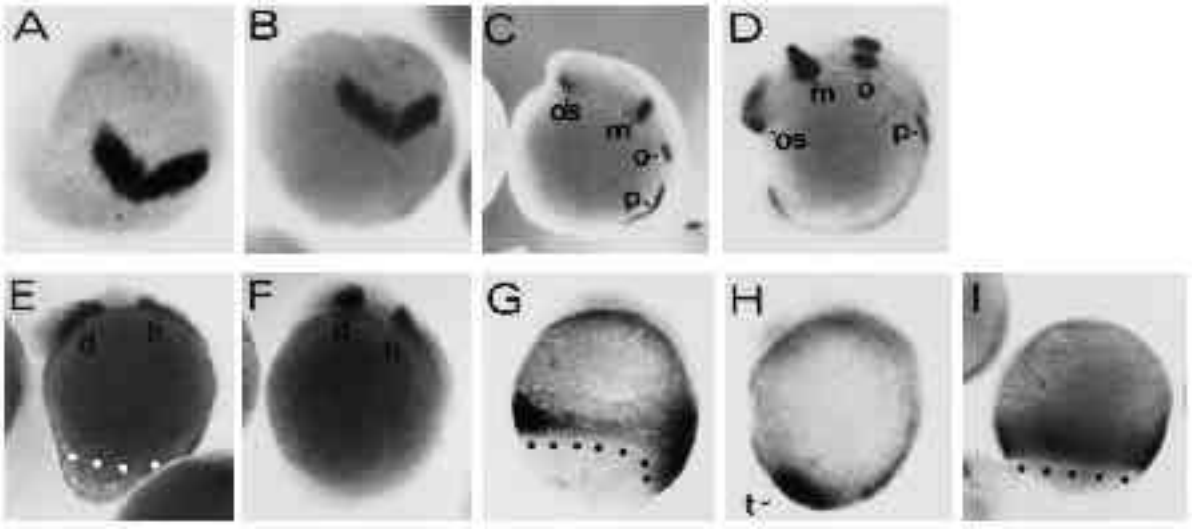

Fig. 7. Regional specification of the body axis in type-A embryos appears to be unaffected by the UV treatment. UV retarded type-A and control embryos were stained with various digoxigenin-labeled RNA probes to assess the regional specification in the truncated axes. (A,B) UV-treated and control embryos at the 2-somite stage stained with an antisense RNA probe directed against the *Zf[pax-b]* gene. Expression of *Zf[pax-b]* is confined to the anlage of the mesencephalon in the neural plate at the 2-somite stage. View onto animal pole is shown, dorsal is at the bottom. (C,D) UV-treated and control embryo at the 8-somite stage labelled with the *Zf[pax-b]* antisense probe. os, optic stalk; m: mesencephalon; o: otic vesicle; p: pronephros. (E,F) UV-treated and untreated control embryo stained with the *ZF[pax-A].* gene. Staining in the diencephalon and the hindbrain is marked by d and h, respectively. (G,H) UV-treated and control embryo at the 4-somite stage. Embryos were stained with the *ZFcad1* probe. t points out the tail bud in control embryo. (I) An 80% epiboly control embryo stained with *ZFcad1* for comparison with staining in G. Embryos, with exception of A and B, are oriented anterior up and dorsal to the right. Blastoderm margins are highlighted by black or white dots. UV embryos were exposed to 3.6 mJ/cm^2 UV.

animal pole (Fig. 6C). For comparison, an *Axial*-stained control sibling (75% epiboly) is shown in Fig. 6D. Fig. 6E and F show *Axial* expression of UV-treated and control embryos fixed when controls had reached the 4-somite stage. *Axial* is expressed at this stage in all three germ layers along the dorsal midline all the way to the animal pole. Similarly, these embryos express the *notail-nonotochord* gene (*ntl*), the zebrafish homologue of the mouse *Brachyury* gene (Schulte-Merker et al., 1992) in the forming notochord (Fig. 6G and H).

In summary, these data show that expression of dorsal gene markers in type-A embryos is unaffected by the UV treatment and that the timing of expression occurs in epiboly-retarded embryos on schedule with untreated controls. The width of the *Axial*- and *ntl*-expressing cell stripe is broader than in controls especially in type-A embryos showing strong retardation of epiboly (compare Fig. 6D and C), suggesting that convergence movements are slightly impaired by the UV treatment. One frequently finds embryos in which the axis shows multiple bends. In these embryos, the presumptive notochord has converged to a similar degree as in controls (compare Fig. 6G and H).

Regional specification of the body axis in UV-retarded embryos

We labeled UV-treated embryos with various probes specific for different anterior-posterior levels of the body axis. The *ZF[pax-b]* gene marks the mesencephalon anlage in early neurula stage embryos. At the 8-somite stage *ZF[pax-b]* is expressed in the optic stalk, the mesencephalon, the otic vesicles and the pronephros (Krausset al., 1991a,b; Püschel et al., 1992b). As shown in Fig. 7A-D, the expression of *ZF[pax-b]* is comparable in UV and control embryos. However, similar to axial mesodermal structures, paraxial mesoderm does not seem to converge to the same degree as in controls since the paired pronephros anlagen are further apart in UV embryos (data not shown). Fig. 7E and F show examples of UV and 8-somite control embryos, respectively, stained with the *ZF[pax-a]* gene marking the diencephalon and the hindbrain (Krauss et al., 1991a,c; Püschel et al., 1992a). Taken together, these data demonstrate that regional specification of the anterior axis is not affected by the UV treatment.

Type-A UV embryos show defects in tail development. The *Zfcad-1* gene labels posterior trunk and tailbud (Joly et al., 1992). As shown in Fig. 7G, *Zfcad-1* is expressed around the blastoderm margin of UV-treated embryos in a manner similar to its expression during gastrulation of normal embryos (see Joly et al., 1992 and Fig. 7I). In addition, *ZFcad-1* seems to be expressed in a tail bud rudiment at the dorsal side resembling expression in the tail bud of an untreated control embryo of the same age (compare Fig. 7G and H). It appears therefore that posterior cell fates are determined in UV embryos. Tail development, however, seems to require blastopore closure, possibly indicating that inductive events between dorsal and ventral cells are required to trigger tail growth.

Detachment of the blastoderm in type-B embryos reveals circumferential forces in the margin

Epiboly is severely inhibited in type-B embryos. The blastoderm spreads so slowly over the yolk sphere that these

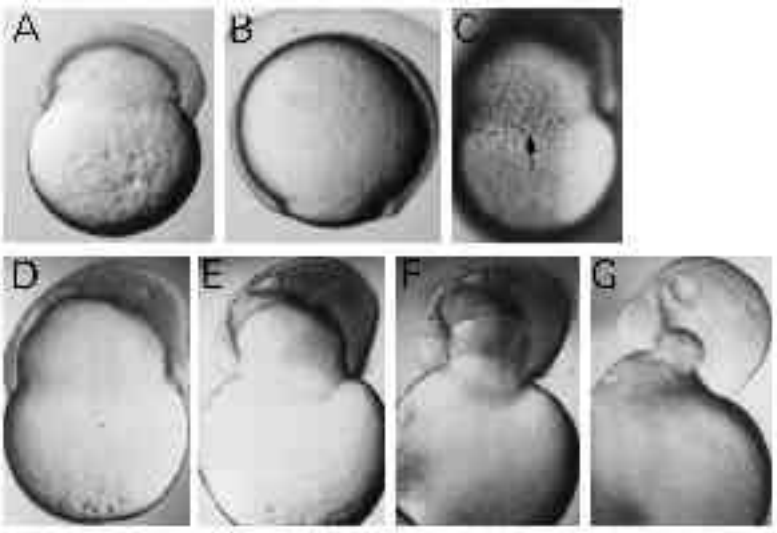

Fig. 8. Type-B embryos constrict off the yolk. (A,B) UV-treated and control embryo of the same age, respectively. UV-treated embryo shows constriction of the yolk cell. Dorsal to the right, anterior up. (C) Circumferentially elongated cells at the margin of the blastoderm in a Type-B embryo (arrow). (D-G) The detachment of the blastoderm from the yolk mass. The frames were taken within 30 minutes.

embryos have not yet reached the 50% epiboly stage when untreated control embryos are closing the blastopore (Fig. 8A,B). The blastoderm of these severely retarded embryos appears to squeeze the yolk cell; an indentation at the blastoderm margin suggests that circumferential forces constrict the yolk mass. During this constriction marginal enveloping layer cells elongate circumferentially as if under considerable stress (Fig. 8C). As a result of the constriction, the blastoderm completely detaches from the yolk mass which, in turn, ruptures. The blastoderm forms a vesicle with a yolk-free centre. The final constriction is a rather rapid process as documented in Fig. 8D-G. Within 30 minutes the blastoderm has cut itself off from the yolk. Although the detachment of the blastoderm from the yolk takes place after control embryos have closed the blastopore, the first signs of constrictive forces around the margin become evident when the blastoderm margin in untreated control embryos passed the equator and started to close the blastopore. This suggests that constriction of the blastoderm margin might be involved in blastopore closure in normal development. In agreement, one finds the yolk forming a plug in UV-treated embryos having passed 50% epiboly, indicating a constrictive force in the blastoderm margin. However, we have never found the exposed yolk in UV-retarded type-A embryos to be sheared off. The actual detachment of the blastoderm from the yolk in type-B embryos might therefore also reflect a weakening of the yolk cytoskeleton by UV treatment.

UV irradiation disrupts microtubules

UV irradiation impairs epiboly irrespective of whether embryos are treated at zygote stages or during epiboly, implying that UV disrupts a component of the machinery driving epiboly that is present from early stages of development. A good candidate for this UV-sensitive component is microtubules. Microtubules and associated motor proteins are known to generate the force necessary for intracellular movements such as vesicular transport, flagellar beat and chromosome segregation (for review see Skoufias and Scholey, 1993 and references therein). Moreover, UV irradiation of *Xenopus* zygotes disrupts microtubules and prevents the microtubule-driven cortical rotation (Elinson and Rowning, 1988).

To determine whether microtubules are disrupted in UV-irradiated zebrafish embryos, we visualized microtubules with the aid of an antibody to β-tubulin. Both treated and untreated embryos, at various stages from the single cell to early epiboly, were examined. Representative results are shown in Fig. 9. In untreated embryos, a network of microtubules was found in the cytoplasmic layer of the yolk cell. This microtubule array, oriented predominantly along the animal-vegetal axis, was present in all stages examined. In embryos where the yolk syncytial layer had formed and started to spread, some microtubules in the yolk cytoplasmic layer appeared continuous with those in the yolk syncytial layer (Fig. 9B,D). The leading edge of the yolk syncytial layer was uneven, with large numbers of microtubules always emanating from regions of the yolk syncytial layer margin that had spread furthest over the yolk. This microtubule network was clearly disrupted in UV-treated embryos. In embryos fixed 10 minutes after irradiation, 25 out of 27 embryos contained abnormal microtubules: either microtubules were not detectable, or they were shorter than normal and not aligned along the A-V axis in the yolk cytoplasmic layer, or they took the form of ‘comet-tails’ (Fig. 9E) which could be seen in the yolk cytoplasm as well as blastomeres. Comet-tails were also seen in 5 out of 22 embryos fixed 2 hours after irradiation. In the remaining embryos, microtubules were seemingly normal, with mitotic asters visible in cells. In contrast to untreated controls, however, treated embryos had fewer microtubules in the cortical layer of the yolk. In 5 out of 6 UV-treated embryos where the yolk syncytial layer had begun spreading, there appeared to be fewer microtubules in the border region between the yolk cytoplasmic layer and the yolk syncytial layer (Fig. 9F compare with D). Microtubules, thus, appear to recover in all regions of the embryo except in the yolk cytoplasm. The reduced density of microtubules in the yolk cytoplasm may account for the slower spread of the blastoderm in UV-treated embryos.

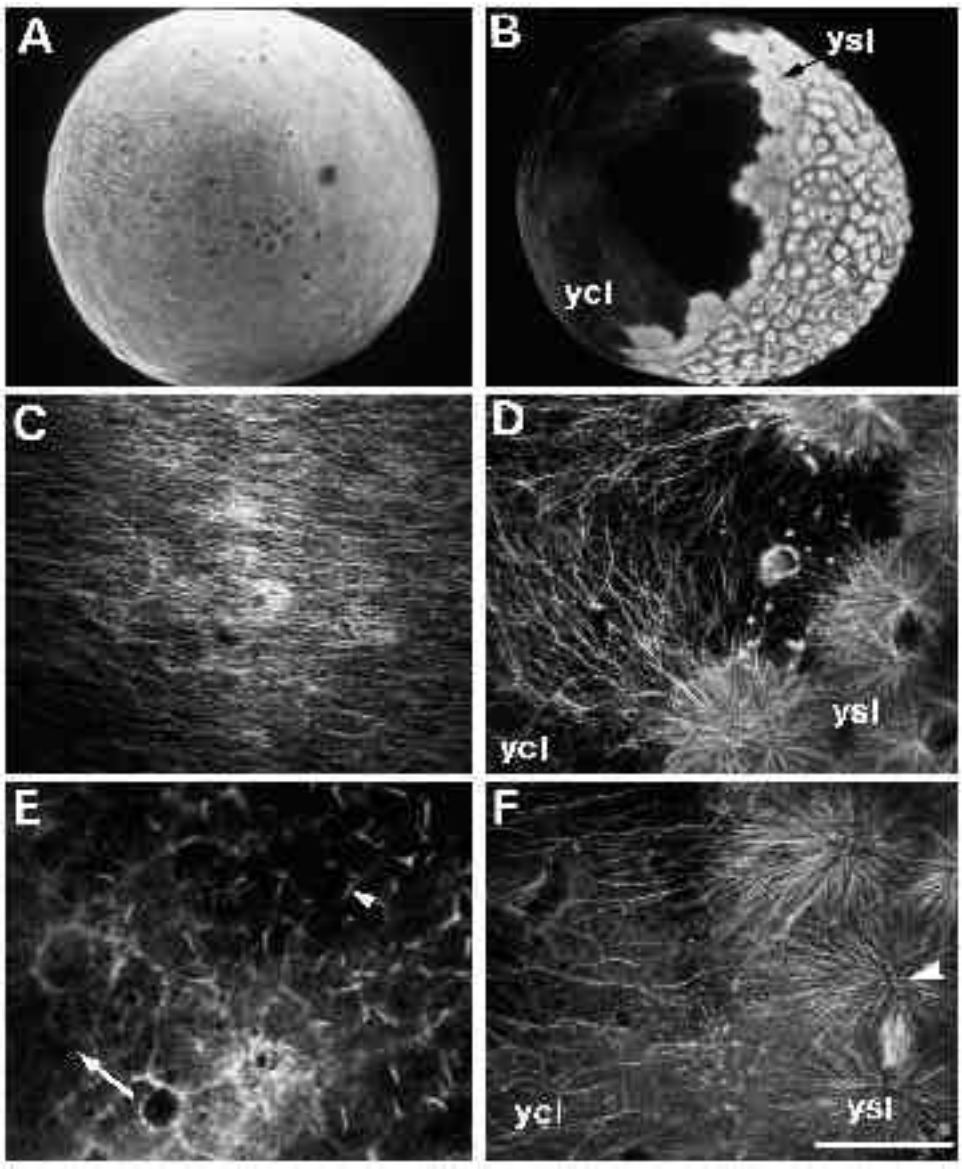

Fig. 9. Immunofluorescent staining of microtubules in untreated (panels A-D) and UV-treated embryos (panels E-F). (A) An untreated embryo, approximately 30 minutes after fertilization. When examined at high magnification (C), a parallel array of microtubules can be seen in the yolk cytoplasmic layer. (B) An untreated embryo at approximately 3.5 hours after fertilization, with a spreading yolk syncytial layer (ysl). Numerous microtubules radiate from the yolk syncytial layer (ysl) into the yolk cytoplasmic layer (ycl), as shown at high magnification in D. Microtubules are disrupted in UV-treated embryos (E,F). In embryos fixed 10 minutes after irradiation, microtubules throughout the embryo appear abnormal. (E) One such embryo, where microtubules in the yolk cytoplasmic layer are either very sparse (arrow) or present in the aberrant form of 'comet-tails' (arrowhead). In embryos fixed 2 hours after irradiation, an example of which is shown in F, some microtubules appear normal, as demonstrated by the mitotic aster in the yolk syncytial layer (arrowhead). In the yolk cytoplasmic layer, however, microtubules are still disrupted: there are far fewer microtubules in the region bordering the yolk syncytial layer (compare with similar region in panel D). Bar, 250 μm (for A,B); 50 μm (for C-F).

Nocodazole mimics effect of UV irradiation

UV irradiation may disrupt other molecules, such as nucleic acids or other proteins besides microtubules. To determine if disrupting microtubules alone is sufficient to mimic the effects of UV irradiation, we briefly incubated embryos in the microtubule-depolymerizing drug nocodazole (Lee et al., 1980). Embryos at cleavage stages were incubated for 10 minutes in 0.6 μg/ml, 1.0 μg/ml or 2.0 μg/ml nocodazole. Treated embryos began epiboly later and progressed through epiboly more slowly than untreated controls. When an untreated embryos was at 50% epiboly (Fig. 10A), for example, a sibling treated with 1 μg/ml nocodazole had reached only 30% epiboly (Fig. 10B). Table 3 summarizes the results when controls reached 100% epiboly. Embryos treated with the 2 μg/ml typically constricted off the yolk, thus resembling type-B UV-treated embryos. With 1 μg/ml, fewer type-B embryos were obtained while strongly retarded type-A embryos, averaging approximately 70% epiboly, were seen in addition. Embryos treated with 0.6 μg/ml were also retarded in epiboly, having reached 80% epiboly at this time. These observations suggest that higher doses of nocodazole cause greater retardation in epiboly. Similar to type-A UV embryos, nocodazole-induced epiboly-retarded embryos develop a distinct axis, as shown in Fig. 10F. The effects of UV irradiation can thus be mimicked by disrupting microtubules only. This strongly supports the notion

Table 3. Effect of incubating cleavage-stage embryos in nocodazole

Nocodazole μg/ml	Normal	Type-A	Type-B
0	10 (100%)	0	0
0.6	0	8 (80%)	2
1.0	0	6 (73%)	5
2.0	0	0	23

Embryos at the 16- to 128-cell stage were bathed in nocodazole for ten minutes and examined when controls reached 100% epiboly. The numbers in parentheses are the average degree of epiboly reached by the embryos.

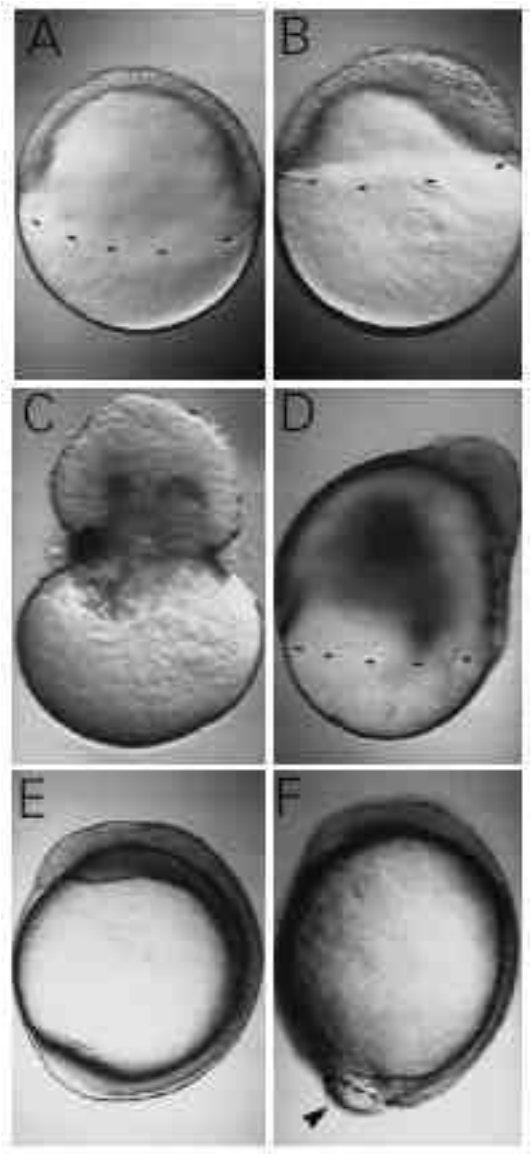

Fig. 10. Nocodazole, a microtubule-depolymerizing agent, mimics the effect of UV. (A) An untreated embryo at 50% epiboly. A sibling, incubated in 1 μg/ml nocodazole, has reached only 30% epiboly (B). (C,D) Observations made at a later stage, when controls have just completed epiboly. 2 μg/ml of nocodazole caused the blastoderm to pinch off the yolk cell (C), while 1 μg/ml caused severe retardation of epiboly (D). At 12 hours after fertilization, when untreated embryos have long finished epiboly (E), an embryo treated with 0.6 μg/ml has still not closed the blastopore (F, arrowhead). Although epiboly is retarded, a distinct axis has formed, with somitogenesis well underway.

that UV disrupts microtubules and that epiboly is impaired by disturbance of microtubule arrays.

DISCUSSION

In this report, we describe the effects of UV irradiation on zebrafish embryos. UV light impairs epiboly regardless of whether the embryo is irradiated during cleavage or during epiboly stages. The velocity of the spread of the blastoderm over the yolk cell is reduced by UV irradiation in a dose-dependent manner. In the majority of embryos, a well-formed anterior axis develops, with various structures such as eyes, neural tube, otic vesicle, somites and notochord clearly visible. We present evidence that UV impairs epiboly by disrupting microtubules in the cortical layer of the yolk cytoplasm.

Gastrulation is independent of epiboly

Genes expressed in restricted domains during gastrulation, such as *ZF[pax-a]* and *ZF[pax-b]*, *ntl*, *Axial* and *Zfcad1*, are all expressed in type-A UV-treated embryos with timings of expression comparable to untreated controls. Retardation of epiboly does not prevent gastrulation. Involution and convergence can occur in UV-treated embryos that have only reached 30% epiboly, when controls are at 50% epiboly, which is the stage where gastrulation normally begins. Gastrulation thus appears to be timed by a clock independent of the degree of epiboly. There appears to be no cues, locally positioned at the equator of the yolk, that induce the gastrulation movements. A cell-intrinsic clock controlling gastrulation is in agreement with the autonomous timing of migratory behaviour of isolated blastomeres of *Fundulus heteroclitus* (Trinkaus, 1963). In *Xenopus laevis* embryos, gastrulation appears to be similarly controlled by a cell-endogenous clock (Cooke and Smith, 1990). The flexibility of timing of gastrulation with respect to epiboly is reflected in the development of various other fishes, such as *Fundulus* and salmon, in which gastrulation is initiated at stages earlier than 50% epiboly (Oppenheimer, 1937; Ballard, 1973b). In general it appears that gastrulation begins earlier with respect to epiboly the larger the egg (Trinkaus, 1984b, 1992).

In *Xenopus*, convergence of involuting and non-involuting cells towards the dorsal side has been shown to drive extension of the body axis and is also thought to drive closure of the blastopore (Keller et al., 1992). Deep cells converge towards the dorsal side in types-A and -B UV-treated embryos forming a distinct thickening at the dorsal margin of the blastoderm cap. Convergence appears to be slightly retarded in comparison to control embryos, as revealed by a wider axis and the broader expression domains of *Axial* and *ntl* in many of the treated embryos. In some embryos that failed to close the blastopore, however, the presumptive notochord had converged to a similar degree as in controls and, very strikingly, these embryos had multiple bends in their axes. Convergence appears to have produced a strong enough force to subject the axes to compression which was then released by bending of the axis. The force produced by convergence is probably what drives extension in the zebrafish; other manifestations of this force can be seen in embryos that have failed to close the blastopore where the yolk becomes stretched to a peanut shape. Convergence drives extension in the fish, but, in contrast to *X. laevis*, it appears to be insufficient to close the blastopore.

UV irradiation and specification of the embryonic axis

In rare cases, embryos lacking any dorsal structures are obtained. These embryos, which we have designated type-

C, appear radially symmetrical. Similar observations have been made by D. Kane (Ho, 1992). Type-C embryos, in addition to lacking dorsal structure, are also impaired in epiboly. They are obtained with greater frequency when staged zygotes are irradiated between 10 and 25 minutes after fertilization, implying that axis specification requires an early, UV-sensitive component. Interestingly, early irradation of *X. laevis* embryos with UV light disrupts cortical rotation, resulting in radially symmetrical ventralized embryos that, in the extreme, lack all anterior and dorsal structures (Malacinsky et al., 1977). In the zebrafish, the nature of early events that specify the axis are unknown. Determination of the future dorsal side by the entry point of the sperm as in *X. laevis* is unlikely since the sperm penetrates the zebrafish egg through a preformed opening in the chorion at the animal pole (Wolensky and Hart, 1987).

The mechanism of epiboly

Based largely on the work of Trinkaus and colleagues in *Fundulus heteroclitus*, there is now strong evidence that epiboly of the teleost blastoderm is dependent on the yolk syncytial layer (Trinkaus, 1984a,b, 1992). To understand the mechanism of epiboly, one thus has to know how the yolk syncytial layer advances. Trinkaus and Oster have proposed that a contractile force at the blastoderm margin, in the yolk syncytial layer, drives epiboly (Trinkaus, 1984b). Contraction in this region is demonstrated by a constriction of the blastoderm margin in *Fundulus* from stage $15\frac{1}{2}$ onwards (Trinkaus, 1951), and by the constriction seen in severely epiboly-retarded type-B zebrafish embryos. This circumferential contraction is probably actin-mediated, as high amounts of actin have been detected in the external yolk syncytial layer (the region between the EVL and the leading margin of the yolk syncytial layer) (Betchaku and Trinkaus, 1978). But circumferential contraction in this layer alone cannot cause it to spread over the equator; on the contrary, contraction on its own will pinch the blastoderm off the yolk. Spreading of the yolk syncytial layer, especially at the initial stages, does not entail circumferential tension - our observation that the leading edge of the yolk syncytial layer is uneven during early stages of spreading indicates that circumferential tension is not predominant. In *Fundulus*, contraction of the external yolk syncytial layer appears to also occur in the animal-vegetal direction, pulling the blastoderm margin closer to the advancing margin of the yolk syncytial layer. This contraction, which has been observed to occur at the onset of blastoderm spreading (Trinkaus, 1951; Betchaku and Trinkaus, 1978), however, cannot in itself cause the yolk syncytial layer to advance towards the vegetal pole. A component outside the yolk syncytial layer, in the yolk cytoplasm, must be involved.

Several lines of evidence prompt us to suggest that the yolk syncytial layer is propelled over the surface of the yolk by microtubule motors that move along microtubule tracks in the yolk cytoplasmic layer. An array of microtubules is present in the yolk cytoplasmic layer from the single-cell stage onwards. After the yolk syncytial layer forms and spreads, many of these microtubules appear to radiate from the margin of the syncytial layer; some microtubules also appear continuous between the yolk syncytial layer and the yolk cytoplasm. The region of the yolk syncytial margin that has advanced furthest always has large numbers of microtubules radiating into the yolk cytoplasmic layer, aligned in the direction of advance. Microtubule motors, perhaps anchored at the margin of the yolk syncytial layer, may drive epiboly by moving on these microtubules. The fact that microtubules are necessary for epiboly is demonstrated by the finding that two microtubule-disrupting agents, UV light and nocodazole, impair epiboly. Cell division continues, indicating that some microtubule function is recovered. Irradiated embryos, however, show reduced amounts of microtubules in the yolk cytoplasm especially at the yolk cytoplasmic layer-yolk syncytial layer border, consistent with the notion that microtubules in this region play a crucial role in epiboly. Moreover, the reduced number of microtubules is consistent with the observation that UV-irradiated embryos epibolize slower than untreated controls. Epiboly can be retarded by UV irradiation even in embryos that have reached 80% epiboly (S. J., unpublished data), suggesting that the microtubule-based motor is necessary for initial as well as later stages of epiboly.

We propose a mechanical model of epiboly that is based on two force-generating mechanisms: microtubule motors in the yolk syncytial layer and actin-mediated contraction at the blastoderm margin. Specifically, we suggest that epiboly is initiated by a mechanism dependent on microtubules in the cortical layer of the yolk. Motors positioned in the yolk syncytial layer use microtubules extending from the external yolk syncytial layer into the yolk cytoplasmic layer as tracks, thereby pulling the tightly anchored blastoderm towards the vegetal pole. Once the equator is crossed, constriction at the blastoderm margin operates in addition to aid closure of the blastopore.

We are especially indebted to Dr P. Ingham, in whose laboratory this work was carried out, for his support and encouragement. We thank Drs S. Schulte-Merker, S. Krauss and J.-P. Joly for probes and antibodies, and Dr J. Lewis for critically reading the manuscript. We are also grateful to Patrick Blader and Emma Burns for technical assistance and members of the DBU for many helpful discussions. U. S. is supported by the Boehringer Ingelheim Fonds and the Deutsche Forschungsgemeinschaft. S. J. is a Rhodes Scholar. This work was supported by the ICRF.

REFERENCES

Ballard, W. W. (1973a). Morphogenetic movements in *Salmo gaidneri Richardson. J. Exp. Zool.* **184**, 381-426.

Ballard, W. W. (1973b). Normal embryonic stages for Salmonid fishes based on *Salmo gairdneri Richardson* and *Salvelius fontinalis (Mitchill)*. *J. Exp Zool.* **184**, 7-26.

Betchaku, T. and Trinkaus, J. P. (1978). Contact relations, surface activity and cortical microfilaments of marginal cells of the enveloping layer and of the yolk syncytial layer and yolk cytoplasmic layers of *Fundulus* before and during epiboly. *J. Exp. Zool.* **206**, 381-426.

Cooke, J. and Smith, J. C. (1990). Measurement of developmental time by cells of early embryos. *Cell* **60**, 891-894.

Devillers, C. (1961). Structural and dynamic aspects of the development of the teleostean egg. *Adv. Morphol.* **1**, 379-429.

Elinson, R. P. and Rowning, B. (1988). A transient array of parallel microtubules in frog eggs: Potential tracks for a cytoplasmic rotation that specifies the dorso-ventral axis. *Dev. Biol.* **128**, 185-197.

Ho, R. K. (1992). Axis formation in the embryo of the zebrafish, *Brachydanio rerio. Sem. Dev. Biol.* **3**, 53-64.

Joly, J.-S., Maury, M., Joly, C., Duprey, P., Boulekbach, H. and

Condamine, H. (1992). Expression of a zebrafish *caudal* homeobox gene correlatres with the establishment of posterior cell lineage at gastrulation. *Differentiation* **50**, 75-87.

Kane, D. A., Warga, R. M. and Kimmel, C. B. (1992). Mitotic domains in the early embryo of the zebrafish. *Nature* **360**, 735-737.

Keller, R., Shih, J. and Domingo, C. (1992). The patterning and functioning of protrusive activity during convergence and extension of the *Xenopus* organizer. *Development* **1992Supplement**, 81-91.

Kimmel, C. B. and Law, R. D. (1985). Cell lineage of zebrafish blastomeres II.Formation of the yolk syncytial layer. *Dev. Biol.* **108**, 86-93.

Kimmel, C. B., Warga, R. M. and Schilling, T. F. (1990). Origin and organisation of the zebrafish fate map. *Development* **108**, 581-594.

Krauss, S., Johannsen, T., Korzh, V., Moens, U., Ericson, J. U. and Fjose, A. (1991c). Zebrafish *pax[zf-a]*; a paired box-containing gene expressed in the neural tube. *EMBO J* **10**, 3609-3619.

Krauss, S., Johansen, T., Khorz, V. and Fjose, A. (1991b). Expression of the zebrafish paired box gene *pax[zf-b]* during early neurogenesis. *Development* **113**, 1193-1206.

Krauss, S., Johansen, T., Korzh, V. and Fjose, A. (1991a). Expression pattern of zebrafish *pax* genes suggest a role in early brain regionalization. *Nature* **353**, 267-270.

Lee, J. C., Field, D. J. and Lee, L. L. Y. (1980). Effects of nocodazole on structures of calf brain tubulin. *Biochem.* **19**, 6209-6215.

Malacinsky, G. M., Brothers, A. J. and Chung, H. M. (1977). Destruction of components of the neural induction system of the amphibian egg with ultraviolet irradiation. *Dev. Biol.* **56**, 24-39.

Oppenheimer, J. M. (1937). The normal stages of *Fundulus heteroclitus*. *Anat. Rec.* **68**, 1-8.

Püschel, A. W., Gruss, P. and Westerfield, M. (1992a). Sequence and expression pattern of *pax-6* are highly conserved between zebrafish and mice. *Development* **114**, 643-651.

Püschel, A. W., Westerfield, M. and Dressler, G. R. (1992b). Comparative analysis of Pax-2 protein distributions during neurulation in mice and zebrafish. *Mech. Dev.* **38**, 197-208.

Schroeder, M. M. and Gard, D. L. (1992). Organization and regulation of cortical microtubules during the first cell cycle of *Xenopus* eggs. *Development* **114**, 699-709.

Schulte-Merker, S., Ho, R. K., Herrmann, B. G. and Nüsslein-Volhard, C. (1992). The protein product of the zebrafish homologue of the mouse *T* gene is expressed in nuclei of the germ ring and the notochord of the early embryo. *Development* **116**, 1021-1032.

Skoufias, D. A. and Scholey, J. M. (1993). Cytoplasmic microtubule-based motor proteins. *Curr. Opin. Cell Biol.* **5**, 95-104.

Strähle, U., Blader, P., Henrique, D. and Ingham, P. (1993). *Axial*, a gene expressed along the developing axis, is misexpressed in cyclops mutant zebrafish embryos. *Genes Dev.* **7**, 1436-1446.

Trinkaus, J. P. (1951). A study of the mechanism of epiboly in the egg of *Fundulusheteroclitus*. *J. Exp. Zool.* **118**, 269-319.

Trinkaus, J. P. (1963). The cellular basis of *Fundulus* epiboly. Adhesivity of blastula and gastrula cells in culture. *Dev. Biol.* **7**, 513-532.

Trinkaus, J. P. (1984a). Mechanism of *Fundulus* epiboly - a current view. *Amer, Zool.* **24**, 673-688.

Trinkaus, J. P. (1984b). *Cells into Organs. The Forces that Shape the Embryo.* Englewood Cliffs, New Jersey: Prentice-Hall Inc.

Trinkaus, J. P. (1992). The midblastula transition, the YSL transition and the onset of gastrulation in *Fundulus*. *Development* **1992 Supplement,** 75-80.

Trinkaus, J. P. and Erickson, C. A. (1983). Protrusive activity, mode and rate of locomotion, and pattern of adhesion of *Fundulus* deep cells during gastrulation. *J. Exp. Zool.* **228**, 41-70.

Warga, R. M. and Kimmel, C. B. (1990). Cell movements during epiboly and gastrulation in zebrafish. *Development* **108**, 569-580.

Westerfield, M. (1993). *The Zebrafish Book.* Eugene, OR: Univ. Oregon Press.

Wolensky, J. S. and Hart, N. H. (1987). Scanning electron microscope studies of sperm incorporation into the zebrafish (*Brachydanio*) Egg. *J. Exp. Zool.* **243**, 259-273.

Wood, A. and Timmermans, L. P. M. (1988). Teleost epiboly: reassessment of deep cell movement in the germ ring. *Development* **102**, 575-585.

(Accepted 23 August 1993)